Comm. Korean Math. Soc. **16** (2001), No. 3, pp. 487–508

A NUMERICAL METHOD FOR CAUCHY PROBLEM USING SINGULAR VALUE DECOMPOSITION

JUNE-YUB LEE AND JEONG-ROCK YOON

ABSTRACT. We consider the Cauchy problem for Laplacian. Using the single layer representation, we obtain an equivalent system of boundary integral equations. We show the singular values of the ill-posed Cauchy operator decay exponentially, which means that a small error is exponentially amplified in the solution of the Cauchy problem. We show the decaying rate is dependent on the geometry of the domain, which provides the information on the choice of numerically meaningful modes. We suggest a pseudo-inverse regularization method based on singular value decomposition and present various numerical simulations.

1. Introduction

Cauchy problem is to find a harmonic extension that matches the potential and the flux prescribed on a subset of the boundary. With an interpretation, this problem is to construct the interior voltage distribution from the partial boundary measurement of the voltage and the current. The problem can be mathematically stated as follows. Let Ω be a bounded domain in $\mathbb{R}^n (n = 2, 3)$ with C^2 boundary. For given two nonempty open subsets Γ_D and Γ_N of $\partial\Omega$, the Cauchy data $f \in H^1(\Gamma_D)$ and $g \in L^2(\Gamma_N)$ are given. Then we are interested in the following Cauchy problem for Laplacian,

$$\begin{aligned} \Delta u &= 0 \qquad \text{in} \quad \Omega, \\ u &= f \qquad \text{on} \quad \Gamma_D, \\ \frac{\partial u}{\partial \nu} &= g \qquad \text{on} \quad \Gamma_N, \end{aligned} \tag{1.1}$$

where ν denotes the outward normal to $\partial\Omega$.

Received March, 15, 2001. Revised April, 28, 2001.
2000 Mathematics Subject Classification: 65N21, 31A25.
Key words and phrases: Ill-conditioned problem, Layer potential, regularization.
The first author was supported by KOSEF under grant no. 2000-1-10300-001-5.

Since the problem is ill-posed, small errors in the data may cause large errors in the solution, thus numerical solvers should be highly accurate and numerically stable [1, 4, 7]. In order to treat ill-posed problems properly, various regularization techniques have been tried such as Tikhonov regularization, spectral cutoff, Morozov's discrepancy principle, and Landweber iteration [3, 5, 6, 10]. The main concern of the regularization techniques is the investigation of the spectral property of the problem such as condition number and singular values. Without spectral information, one may fail to obtain reasonable approximated solution of the ill-posed problem even with tiny error in the data.

In this paper, we intend to present the essential nature of the spectral property of Cauchy problem. Based on the singular value decomposition, we propose a numerical method using the natural pseudo-inverse with spectral cutoff. The way of spectral cutoff will be controlled by the order of the observation error in the data and how precise solution is expected.

In section 2, the equivalent single layer potential representation of Cauchy problem is presented. And we show that the original Cauchy problem is converted into a system of boundary integral equations for finding charge density without affecting any change in the ill-posedness. In section 3, we mention a numerical method used in the computation of singular system. To maintain high precision in numerical examples, a super algebraic convergent algorithm is required. In section 4, we investigate the singular system of the Cauchy problem in case when the domain is assumed to be an annulus in $\mathbb{R}^2$. We conclude the singular values consist of *standing modes* and *vanishing modes*, and the singular values in vanishing modes decay exponentially. Moreover, the base of exponent is shown to be determined by the geometric property of the domain. In section 5, numerical methods to solve Cauchy problem and some examples are presented.

2. Single layer representation of Cauchy problem

It is well-known that the Cauchy problem (1.1) has a unique solution u in $H^{3/2}(\Omega)$, and u has the following single layer representation for a charge density $\sigma \in L^2(\partial\Omega)$,

$$u(x) = \int_{\partial\Omega} \Phi(x,y)\sigma(y)\, ds_y, \qquad x \in \Omega, \tag{2.1}$$

where Φ is the fundamental solution of Laplacian given by

$$\Phi(x,y) = \frac{1}{2\pi}\log|x-y| \quad \text{if } n=2, \quad \Phi(x,y) = \frac{-1}{4\pi}\frac{1}{|x-y|} \quad \text{if } n=3.$$

With the aid of jump relations for the single layer potential, we get

$$\begin{aligned} &\mathcal{S}_\Omega[\sigma](x) = f(x), \quad x \in \Gamma_D, \\ &\left(-\frac{1}{2}I + \mathcal{K}_\Omega^*\right)[\sigma](x) = g(x), \quad x \in \Gamma_N, \end{aligned} \tag{2.2}$$

where I denotes the identity operator, $\mathcal{S}_\Omega$ and $\mathcal{K}_\Omega^*$ are defined by

$$\mathcal{S}_\Omega[\sigma](x) = \int_{\partial\Omega} \Phi(x,y)\sigma(y)\,ds_y \text{ and } \mathcal{K}_\Omega^*[\sigma](x) = \int_{\partial\Omega} \frac{\partial\Phi(x,y)}{\partial\nu(x)}\sigma(y)ds_y.$$

THEOREM 2.1. *The Cauchy problem* (1.1) *is equivalent to the system of boundary integral equations* (2.2). *Moreover, the solution* $u \in H^{3/2}(\Omega)$ *of* (1.1) *and the solution* $\sigma \in L^2(\partial\Omega)$ *of* (2.2) *satisfy*

$$||u||_{H^{3/2}(\Omega)} \le c_1||\sigma||_{L^2(\partial\Omega)} \quad \text{and} \quad ||\sigma||_{L^2(\partial\Omega)} \le c_2||u||_{H^{3/2}(\Omega)}, \tag{2.3}$$

for some positive constants c_1 *and* c_2.

PROOF. Suppose that $\sigma \in L^2(\partial\Omega)$ solves the boundary integral equations (2.2). Let u be defined by (2.1). With the aid of jump relations for the single layer potential, we easily see that u solves the Cauchy problem (1.1). Moreover, by the well-posedness of Dirichlet boundary value problem we obtain

$$||u||_{H^{3/2}(\Omega)} \le c||u||_{H^1(\partial\Omega)},$$

for a positive constant c. By the representation of (2.1) and the well-known property of single layer potential, we get

$$||u||_{H^1(\partial\Omega)} \le ||\mathcal{S}_\Omega[\sigma]||_{H^1(\partial\Omega)} \le ||\mathcal{S}_\Omega||\,||\sigma||_{L^2(\partial\Omega)}. \tag{2.4}$$

The last inequality of (2.4) is based on the fact that the operator $\mathcal{S}_\Omega$ is bounded from $L^2(\partial\Omega)$ into $H^1(\partial\Omega)$. Hence letting $c_1 := c||\mathcal{S}_\Omega||$, we prove the first part of (2.3).

On the contrary, suppose that $u \in H^{3/2}(\Omega)$ is the solution of the Cauchy problem (1.1). Let $\sigma \in L^2(\partial\Omega)$ be the solution of

$$\mathcal{S}_\Omega[\sigma] = u|_{\partial\Omega} \quad \text{in} \quad H^1(\partial\Omega), \tag{2.5}$$

which is uniquely solvable, since the operator $\mathcal{S}_\Omega : L^2(\partial\Omega) \to H^1(\partial\Omega)$ is invertible. By the uniqueness of the Dirichlet boundary value problem,

u and σ are related by (2.1). Hence σ satisfies (2.2). From (2.5), we have

$$||\sigma||_{L^2(\partial\Omega)} \leq ||\mathcal{S}_\Omega^{-1}||\,||u||_{H^1(\partial\Omega)}.$$

By the trace theorem, we see that $||u||_{H^1(\partial\Omega)} \leq \tilde{c}||u||_{H^{3/2}(\Omega)}$. Hence if we define $c_2 := \tilde{c}||\mathcal{S}_\Omega^{-1}||$, the second part of (2.3) is proved. This completes the proof. □

From (2.2), we can define the *Cauchy operator*

$$\mathcal{C} : L^2(\partial\Omega) \to H^1(\Gamma_D) \times L^2(\Gamma_N) \tag{2.6}$$

by the following system of operators

$$\mathcal{C}[\sigma] := \begin{pmatrix} \mathcal{S}_\Omega[\sigma]|_{\Gamma_D} \\ \left(-\frac{1}{2}I + \mathcal{K}_\Omega^*\right)[\sigma]\big|_{\Gamma_N} \end{pmatrix}. \tag{2.7}$$

By Theorem 2.1, our Cauchy problem (1.1) is converted into the problem for finding the charge density $\sigma \in L^2(\partial\Omega)$ satisfying

$$\mathcal{C}[\sigma] = \begin{pmatrix} f \\ g \end{pmatrix}. \tag{2.8}$$

Since the above system of the boundary integral equations is an ill-posed problem, a numerically stable and accurate method should be applied to obtain a solution of (2.8). In the following section, we consider a numerical method to discretize the integral equations (2.8).

3. Numerical evaluation of Cauchy matrix

In order to compute the system of boundary integral equations (2.8) numerically, we need to pay special attention to each of kernels since the kernels have (weak) singularities and the Cauchy operator is an ill-posed operator (see [2]). First we consider a numerical quadrature for the operator $\mathcal{K}_\Omega^*$ by looking at the limiting value of the kernel $\partial\Phi(x,y)/\partial\nu(x)$. The following lemma can be proved by simple straightforward calculation, thus we omit the proof.

LEMMA 3.1. *Let Ω be a bounded domain in $\mathbb{R}^2$ with C^2 boundary. Then the kernel $\partial\Phi(x,y)/\partial\nu(x)$ of the integral operator $\mathcal{K}_\Omega^*$ has a removable singularity as y approaches $x \in \partial\Omega$ along the boundary $\partial\Omega$. In*

fact, the limit is expressed by

$$\lim_{y\to x}\frac{\partial \log|x-y|}{\partial \nu(x)} = \frac{1}{2}\kappa(x) \tag{3.1}$$

where κ is the signed curvature of $\partial\Omega$. Thus, the smoothness of the kernel of $\mathcal{K}^*_\Omega$ is limited only by the smoothness of $\partial\Omega$. For infinitely differentiable curves, the kernel is infinitely differentiable.

Let $\Omega \subset \mathbb{R}^2$ be a bounded domain and suppose that $\partial\Omega$ consists of K disjoint smooth boundary segments $\partial\Omega = \bigcup_{k=1}^{K}\Gamma_k$. We select N_k points $\{y_j^k\}_{j=1}^{N_k}$ on Γ_k of the k-th boundary segment which are equi-spaced in terms of arc-length and define $h_k = |\Gamma_k|/N_k$, where $|\Gamma_k|$ denotes the arc-length of Γ_k. Associated with each point $y_j^k \in \Gamma_k$, let σ_j^k denote the charge density $\sigma(y)$ at $y = y_j^k$. Then

$$\mathcal{K}^*_\Omega[\sigma](x) = \int_{\partial\Omega}\frac{\partial\Phi(x,y)}{\partial\nu(x)}\sigma(y)ds_y$$

can be approximated at each $x_i^l \in \Gamma_l$, $i = 1,\cdots,N_l$ and $l = 1,\cdots,K$ using the trapezoidal rule by

$$K^*\{\sigma_j^k\}(x_i^l) := \frac{1}{2\pi}\sum_{k=1}^{K} h_k \sum_{j=1}^{N_k}\sigma_j^k \frac{\partial \log|x_i^l - y_j^k|}{\partial\nu(x_i^l)}, \tag{3.2}$$

where $\partial\log|x_i^l - y_j^k|/\partial\nu(x_i^l)$ should be replaced by $\frac{1}{2}\kappa(x_i^l)$ for $y_j^k = x_i^l$ with the aid of Lemma 3.1.

LEMMA 3.2. *Suppose that $\{x_i^l\}_{i=1}^{N_l}$ are points on each smooth boundary segment Γ_l, $l = 1,\cdots,K$ and located equally in terms of arc-length. Then $K^*\{\sigma_j^k\}(x_i^l)$ defined in (3.2) converges super-algebraically to $\mathcal{K}^*_\Omega[\sigma](x_i^l)$.*

PROOF. The proof is a direct application of Euler-McLaurin's formula for a function $f \in C^{(2m)}[a,b]$ with uniform grid points $x_j = a + jh$ for $j = 1,\cdots,n$ and $h = (b-a)/n$,

$$h\sum_{j=1}^{n} f(x_j) = \int_a^b f(x)dx + \frac{h}{2}f(x)\Big|_a^b + \sum_{l=1}^{m-1} h^{2l}\frac{B_{2l}}{(2l)!}\, f^{(2l-1)}(x)\Big|_a^b + R_{2m},$$

where B_{2l} denotes the l-th order Bernoulli number and

$$R_{2m} = h^{2m}\frac{B_{2m}}{(2m)!}(b-a)f^{(2m)}(\xi) \quad \text{for some} \quad a \le \xi \le b.$$

Since the intermediate terms $f^{(2l-1)}(x)\big|_{x=a}^{x=b}$ vanish for smooth periodic function f, the trapezoidal rule has an error

$$h^{2m}\frac{B_{2m}}{(2m)!}(b-a)\max_{a\le\xi\le b}|f^{(2m)}(\xi)|$$

which decays super algebraically. □

In order to compute the single layer potential

$$\mathcal{S}_\Omega[\sigma](x)=\int_{\partial\Omega}\Phi(x,y)\sigma(y)\,ds_y$$

maintaining high accuracy, one may apply a similar technique used in (3.2) for the evaluation of $K_\Omega^*[\sigma]$, that is,

$$S\{\sigma_j^k\}(x_i^l):=\frac{1}{2\pi}\sum_{k=1}^{K}h_k\sum_{j=1}^{N_k}\sigma_j^k\,\log|x_i^l-y_j^k|,$$

where σ_j^k denotes the charge density $\sigma(y)$ at $y=y_j^k$. Although the single layer potential has an integrable singularity at $y=x$, the corresponding term in the summation can not be evaluated at $y_j^k=x_i^l$. To avoid such a difficulty, we divide the boundary points $\{y_j^k\}$ into two classes, so called *odd* and *even* points. The values $S\{\sigma_j^k\}$ at odd points are obtained using the trapezoidal rule with sources $\sigma(y)$ at even points $y=y_j^k$ and those at even points are obtained with source data at odd points $y=y_j^k$. Hence we have

$$S\{\sigma_j^k\}(x_i^l):=\frac{1}{\pi}\sum_{k=1}^{K}h_k\sum_{y_j^k\in Y_p}\sigma_j^k\,\log|x_i^l-y_j^k|, \tag{3.3}$$

where Y_p is the set of even (or odd) points if x_i^l is an odd (or even) point. It can be shown that such a rule is super-algebraically convergent on a smooth domain Ω. (See [8, 9].) Incorporating (3.3) with (3.2), we get the following theorem.

THEOREM 3.3. *Let $\{\sigma_j\}_{j=1}^n$ be the charge density data on n equally spaced points $\{y_j\}_{j=1}^n$ on a smooth boundary $\partial\Omega$. Let $\{x_i\}_{i=1}^{m_D}$ be m_D points on $\Gamma_D\subset\partial\Omega$ where Dirichlet data are specified and $\{x_i\}_{i=m_D+1}^{m_D+m_N}$*

be m_N points on the Neumann boundary segments $\Gamma_N \subset \partial\Omega$. The $(m_D + m_N) \times n$ Cauchy matrix C is defined as follows:

$$C_{ij} = \begin{pmatrix} S\{\sigma_j\}(x_i) & \text{defined in (3.3)} & \text{if } i \le m_D \\ K^*\{\sigma_j\}(x_i) & \text{defined in (3.2)} & \text{if } i > m_D \end{pmatrix} \tag{3.4}$$

for $i = 1, \cdots, m_D + m_N$ and $j = 1, \cdots, n$. Then, $C\{\sigma_j\}$ converges super-algebraically to $\mathcal{C}[\sigma]$ at target points $\{x_i\}_{i=1}^{m_D+m_N}$ as n, m_N, and m_D increases.

Now we are in a position to calculate the singular system of the Cauchy operator $\mathcal{C}$ using the Cauchy matrix C. It is numerically possible to compute singular values and singular vectors corresponding to the Cauchy operator $\mathcal{C}$ defined from $L^2(\partial\Omega)$ into $H^1(\Gamma_D) \times L^2(\Gamma_N)$, however, it is more convenient to view the Cauchy operator as

$$\mathcal{C} : L^2(\partial\Omega) \to L^2(\Gamma_D) \times L^2(\Gamma_N), \tag{3.5}$$

when the Cauchy data are given in the form of pointwise values.

Since the norms in $H^1(\Gamma_D)$ and $L^2(\Gamma_D)$ are related by

$$||f||_{L^2(\Gamma_D)} \le ||f||_{H^1(\Gamma_D)} \le (1 + m_D^2)^{1/2} ||f||_{L^2(\Gamma_D)},$$

the ratio of two norms is bounded by the highest frequency m_D of f. Therefore, corresponding singular values of the Cauchy operator defined in (2.6) and (3.5) differ only by an algebraic factor. Hence, the choice of the target space of $\mathcal{C}$ does not make a significant effect on the decaying rate of singular values which is an essential factor to design an optimal numerical solver of the Cauchy problem, as long as the singular values are decaying exponentially. In Theorem 4.3 and Remark 4.5 for the case of annuli in the following section, we will show the singular values of the Cauchy operator decay exponentially both in $L^2(\Gamma_D) \times L^2(\Gamma_N)$ and in $H^1(\Gamma_D) \times L^2(\Gamma_N)$.

Once we consider $\mathcal{C}$ as defined in (3.5), its singular system can be easily computed using singular decomposition method such as QR iteration or Jacobi method from the numerically computed Cauchy matrix (3.4).

4. Singular value decomposition in annuli

The system of boundary integral equations (2.8) equivalent to our Cauchy problem (1.1) is unfortunately an ill-posed problem. In order to deal with ill-posed problems appropriately, we need investigate the

spectral property of the Cauchy operator $\mathcal{C}$ such as condition number $||\mathcal{C}||\,||\mathcal{C}^{-1}||$ and the decaying rate of singular values.

To investigate the nature of the spectral property of $\mathcal{C}$, we take an annulus as an example. This simplest example provides the essential nature of Cauchy problem, and the case of more general domains will be numerically considered in section 5.

Let $\Omega = B_R \setminus \bar{B}_r$ be an annulus in $\mathbb{R}^2$ for some $R > r > 0$, where B_s denotes a disk centered at the origin with radius s. And let $\Gamma_D = \Gamma_N = \partial B_R$. Then the Cauchy problem (1.1) is restated as

$$\begin{aligned} \Delta u &= 0 && \text{in } B_R \setminus \bar{B}_r, \\ u &= f && \text{on } \partial B_R, \\ \frac{\partial u}{\partial \nu} &= g && \text{on } \partial B_R. \end{aligned} \tag{4.1}$$

In this section, we analytically calculate the singular system of the Cauchy operator

$$\mathcal{C} : L^2(\partial\Omega) \to L^2(\partial B_R) \times L^2(\partial B_R)$$

defined in the same manner as in (2.7).

LEMMA 4.1. *Let $\Omega = B_R \setminus \bar{B}_r$ in $\mathbb{R}^2$ and $\Gamma_D = \Gamma_N = \partial B_R$. For a given $\sigma \in L^2(\partial\Omega)$, the image of Cauchy operator*

$$\begin{pmatrix} f(\theta) \\ g(\theta) \end{pmatrix} := \mathcal{C}[\sigma](R\cos\theta, R\sin\theta)$$

is expressed by

$$\begin{aligned} f(\theta) = {} & A_0(R\log R) - \frac{R}{2}\sum_{m=1}^{\infty}\left\{\frac{A_m}{m}\cos m\theta + \frac{B_m}{m}\sin m\theta\right\} \\ & + a_0(r\log R) - \frac{r}{2}\sum_{m=1}^{\infty}\left\{\frac{a_m}{m}\left(\frac{r}{R}\right)^m\cos m\theta + \frac{b_m}{m}\left(\frac{r}{R}\right)^m\sin m\theta\right\}, \\ g(\theta) = {} & -\frac{1}{2}\sum_{m=1}^{\infty}\{A_m\cos m\theta + B_m\sin m\theta\} \\ & + \frac{r}{R}\left[a_0 + \frac{1}{2}\sum_{m=1}^{\infty}\left\{a_m\left(\frac{r}{R}\right)^m\cos m\theta + b_m\left(\frac{r}{R}\right)^m\sin m\theta\right\}\right], \end{aligned}$$

where $\{A_m, B_m\}$ and $\{a_m, b_m\}$ are Fourier coefficients of $\sigma|_{\partial B_R}$ and $\sigma|_{\partial B_r}$, respectively.

PROOF. By (2.2), for $x \in \partial B_R$ and the following series expansions

$$\log|x-y| = \log|x| - \sum_{n=1}^{\infty} \frac{1}{n}\frac{|y|^n}{|x|^n}\cos n\phi,$$

$$\frac{(x-y,x)}{|x||x-y|^2} = \begin{cases} \dfrac{1}{|x|} + \displaystyle\sum_{n=1}^{\infty} \frac{|y|^n}{|x|^{n+1}}\cos n\phi & \text{if } |x| > |y|, \\ \dfrac{1}{2|x|} & \text{if } |x| = |y|, \end{cases}$$

where ϕ is the angle between x and y, the assertions are easily verified by using Fourier coefficients of σ on ∂B_R and ∂B_r. This completes the proof. □

In Lemma 4.1, we can see that the coefficients related to the Fourier coefficients $\{a_m, b_m\}$ on the inner boundary are exponentially decreasing with the base (r/R) as m goes to infinity, while those related to the Fourier coefficients $\{A_m, B_m\}$ on the outer boundary are not. This fact will be the main reason why the singular values of C decay exponentially.

Consider the natural Fourier orthonormal basis in $L^2(\partial\Omega)$ such as charge densities $\{\sigma_R^m, \varsigma_R^m\}$ supported on ∂B_R, and $\{\sigma_r^m, \varsigma_r^m\}$ supported on ∂B_r, whose parametizations are given by

$$\sigma_R^0|_{\partial B_R} = \frac{1}{\sqrt{2\pi R}}, \qquad \sigma_R^m|_{\partial B_R} = \frac{\cos m\theta}{\sqrt{\pi R}}, \qquad \varsigma_R^m|_{\partial B_R} = \frac{\sin m\theta}{\sqrt{\pi R}},$$

$$\sigma_r^0|_{\partial B_r} = \frac{1}{\sqrt{2\pi r}}, \qquad \sigma_r^m|_{\partial B_r} = \frac{\cos m\theta}{\sqrt{\pi r}}, \qquad \varsigma_r^m|_{\partial B_r} = \frac{\sin m\theta}{\sqrt{\pi r}}.$$

By Lemma 4.1 the corresponding images of Cauchy operator are given by

$$\begin{aligned} &C[\sigma_R^0] = (R\log R)\varphi_R^0, && C[\sigma_r^0] = \sqrt{1+(R\log R)^2}\left(\frac{r}{R}\right)^{1/2}\varphi_r^0, \\ &C[\sigma_R^m] = \tau_m\varphi_R^m, && C[\sigma_r^m] = \tau_m\left(\frac{r}{R}\right)^{m+1/2}\varphi_r^m, \\ &C[\varsigma_R^m] = \tau_m\psi_R^m, && C[\varsigma_r^m] = \tau_m\left(\frac{r}{R}\right)^{m+1/2}\psi_r^m, \end{aligned} \tag{4.2}$$

where $\tau_m = \frac{1}{2}\sqrt{1+(R/m)^2}$ and φ_R^m, ψ_R^m, φ_r^m and ψ_r^m are defined by

$$\varphi_R^0 = \left(\frac{1}{\sqrt{2\pi R}}, 0\right), \qquad \varphi_r^0 = \frac{1}{\sqrt{1+(R\log R)^2}}\left(\frac{R\log R}{\sqrt{2\pi R}}, \frac{1}{\sqrt{2\pi R}}\right),$$

$$\varphi_R^m = \left(\frac{-R\sigma_R^m}{\sqrt{m^2+R^2}}, \frac{-m\sigma_R^m}{\sqrt{m^2+R^2}}\right), \quad \varphi_r^m = \left(\frac{-R\sigma_R^m}{\sqrt{m^2+R^2}}, \frac{m\sigma_R^m}{\sqrt{m^2+R^2}}\right),$$

$$\psi_R^m = \left(\frac{-R\varsigma_R^m}{\sqrt{m^2+R^2}}, \frac{-m\varsigma_R^m}{\sqrt{m^2+R^2}}\right), \quad \psi_r^m = \left(\frac{-R\varsigma_R^m}{\sqrt{m^2+R^2}}, \frac{m\varsigma_R^m}{\sqrt{m^2+R^2}}\right).$$

With the above consideration,

$$\Sigma := \{\sigma_R^0, \sigma_R^m, \varsigma_R^m, \sigma_r^0, \sigma_r^m, \varsigma_r^m\}_{m\geq 1} \tag{4.3}$$

constitutes a complete orthonormal system in $L^2(\partial\Omega)$ and each element in

$$\Psi := \{\varphi_R^0, \varphi_R^m, \psi_R^m, \varphi_r^0, \varphi_r^m, \psi_r^m\}_{m\geq 1} \tag{4.4}$$

has a unit norm, but is not an orthonormal system in $L^2(\partial B_R) \times L^2(\partial B_R)$, since we have

$$\langle \varphi_R^0, \varphi_r^0 \rangle = \frac{R\log R}{\sqrt{1+(R\log R)^2}}, \tag{4.5}$$

$$\langle \varphi_R^m, \varphi_r^m \rangle = \langle \psi_R^m, \psi_r^m \rangle = -\frac{m^2-R^2}{m^2+R^2}, \tag{4.6}$$

where $\langle \cdot, \cdot \rangle$ denotes the inner product in $L^2(\partial B_R) \times L^2(\partial B_R)$.

Therefore, to obtain the singular system we require a standard Gram-Schmidt orthogonalization procedure. Because this procedure is easy but tedious, we leave it to Appendix A. By virtue of Theorem A.1, we obtain $\bar{\Sigma}$ and $\bar{\Psi}$ that are respectively orthonormal systems in $L^2(\partial\Omega)$ and $L^2(\partial B_R)\times L^2(\partial B_R)$, and the corresponding singular values $\{\bar{\mu}_R^m, \bar{\mu}_r^m\}_{m\geq 0}$ are also obtained.

From the singular values of $\mathcal{C} : L^2(\partial\Omega) \to L^2(\partial B_R) \times L^2(\partial B_R)$ calculated in Theorem A.1, we observe that there are two kinds of modes such as

$$\text{Standing modes} = \left\{(\bar{\mu}_R^m, \bar{\sigma}_R^m, \bar{\varphi}_R^m), (\bar{\mu}_R^m, \bar{\varsigma}_R^m, \bar{\psi}_R^m)\right\}_{m\geq 0},$$

$$\text{Vanishing modes} = \left\{(\bar{\mu}_r^m, \bar{\sigma}_r^m, \bar{\varphi}_r^m), (\bar{\mu}_r^m, \bar{\varsigma}_r^m, \bar{\psi}_r^m)\right\}_{m\geq 0}.$$

Using the numerical method described in section 3, we compute the singular system of the Cauchy matrix defined in (3.4).

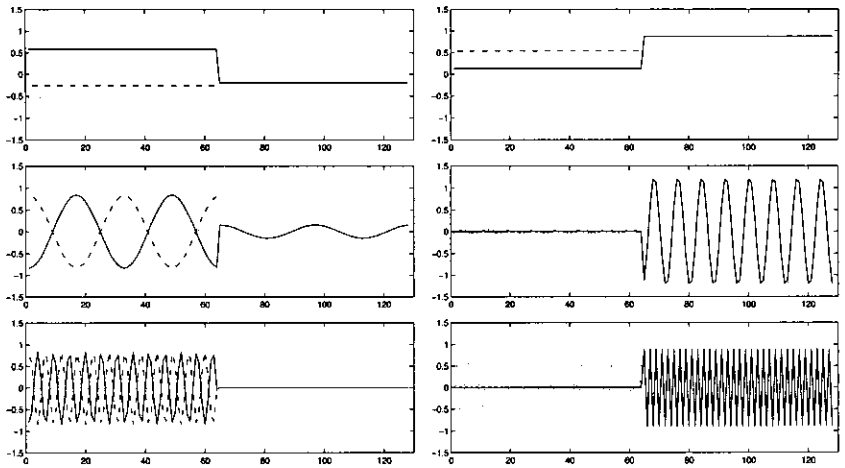

(a) (b)

FIGURE 1. Solid line for charge density, dotted line for potential, and dash-dotted line for flux are drawn when $R = 0.45$ and $r = 0.20$. (a) Standing modes $(\bar{\sigma}_R^m, \bar{\varphi}_R^m)$ when $m = 0, 2, 12$. (b) Vanishing modes $(\bar{\sigma}_r^m, \bar{\varphi}_r^m)$ when $m = 0, 8, 31$.

EXAMPLE 4.2. We select equi-spaced 64 points on the outer boundary $\partial B_{0.45}$ and the inner boundary $\partial B_{0.20}$, respectively. Then we obtain 128 modes in the singular system. In Figure 1, we present some standing modes and vanishing modes. The horizontal axis represents the ordering of boundary points: the points numbered within $1, \cdots, 64$ represent those on the outer boundary $\partial B_{0.45}$ with counter-clockwise ordering, and the points numbered within $65, \cdots, 128$ represent those on the inner boundary $\partial B_{0.25}$ in the same manner. The solid line represents the charge densities $\bar{\sigma}_R^m$ and $\bar{\sigma}_r^m$ $(R = 0.45,\ r = 0.20)$, the dotted line represents the potential part of $\bar{\varphi}_R^m$ and $\bar{\varphi}_r^m$, and the dash-dotted line represents the flux part of $\bar{\varphi}_R^m$ and $\bar{\varphi}_r^m$.

We can observe that the charge densities in standing modes are *mainly supported* on the outer boundary $\partial B_{0.45}$ and those of vanishing modes are *mainly supported* on the inner boundary $\partial B_{0.20}$. Here we mean that $\sigma \in L^2(\partial\Omega)$ is *mainly supported* on ∂B_R if $||\sigma||_{L^2(\partial B_R)} \gg ||\sigma||_{L^2(\partial B_r)}$ and is *mainly supported* on ∂B_r if $||\sigma||_{L^2(\partial B_R)} \ll ||\sigma||_{L^2(\partial B_r)}$. In the proof of the following Theorem 4.3, we will obtain that $c_m =$

$O((r/R)^m)$, which implies that $\bar{\sigma}_R^m$ and $\bar{\varsigma}_R^m$ are actually mainly supported on ∂B_R, while $\bar{\sigma}_r^m$ and $\bar{\varsigma}_r^m$ are mainly supported on ∂B_r, by virtue of their own definitions in Theorem A.1. As m increases, we observe that $\{\bar{\sigma}_R^m, \bar{\varsigma}_R^m\}$ and $\{\bar{\sigma}_r^m, \bar{\varsigma}_r^m\}$ are almost same as $\{\sigma_R^m, \varsigma_R^m\}$ and $\{\sigma_r^m, \varsigma_r^m\}$, respectively.

In the following theorem, we will show that the standing modes remain actually bounded, and the vanishing modes decay exponentially as we may imagine from their names. And it is a natural conclusion from the physical viewpoint if we think of the potential and flux induced by an oscillatory boundary charge density.

THEOREM 4.3. *Under the same assumption in Lemma 4.1 with $R < 1$, the singular values of $\mathcal{C} : L^2(\partial\Omega) \to L^2(\partial B_R) \times L^2(\partial B_R)$ decay exponentially. That is, the singular values $\{\bar{\mu}_R^m, \bar{\mu}_r^m\}_{m\geq 0}$ have the following asymptotic behavior,*

$$\bar{\mu}_R^m = O(1) \quad \text{and} \quad \bar{\mu}_r^m = O\left(\left(\frac{r}{R}\right)^m\right). \tag{4.7}$$

PROOF. Solving (A.2) and choosing the negative solution, we get

$$c_m = -\frac{m^2+R^2}{m^2-R^2}\left(\frac{r}{R}\right)^{m+1/2} + \frac{8m^2R^2}{m^4-R^4}\left(\frac{r}{R}\right)^{m+1/2}\left(1+\left(\frac{r}{R}\right)^{2m+1}\right)^{-1} \times \left(1+\sqrt{1-\frac{16m^2R^2}{(m^2+R^2)^2\left(\left(\frac{r}{R}\right)^{m+1/2}+\left(\frac{R}{r}\right)^{m+1/2}\right)^2}}\right)^{-1}$$

implies $c_m = O((r/R)^m)$. By Theorem A.1,

$$\bar{\mu}_R^m = \frac{\tau_m\beta_m}{\alpha_m} = \frac{1}{2}\sqrt{\frac{1+(R/m)^2}{1+O\left((r/R)^{2m}\right)}}\sqrt{1+O\left(\left(\frac{r}{R}\right)^{2m}\right)}$$

proves the first part of (4.7). On the other hand, $\bar{\mu}_r^m$ has the following asymptotic behavior

$$\bar{\mu}_r^m = \frac{\tau_m\gamma_m}{\alpha_m} = \frac{1}{2}\sqrt{\frac{1+(R/m)^2}{1+O\left((r/R)^{2m}\right)}}\,O\left(\left(\frac{r}{R}\right)^m\right),$$

which proves the second part of (4.7). □

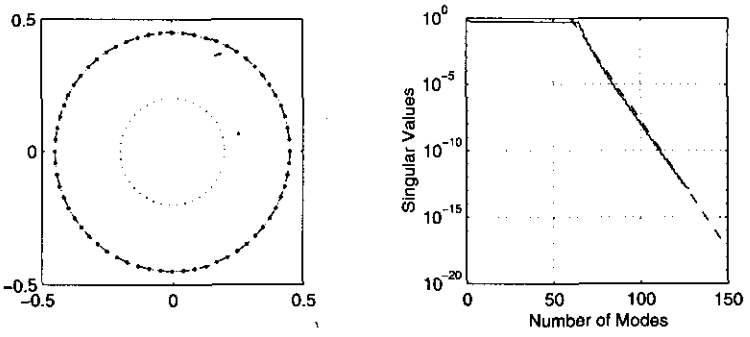

FIGURE 2. $\Omega = B_{0.45} \setminus \bar{B}_{0.2}$ with Cauchy data on $\partial B_{0.45}$ and its corresponding singular values in Example 4.4.

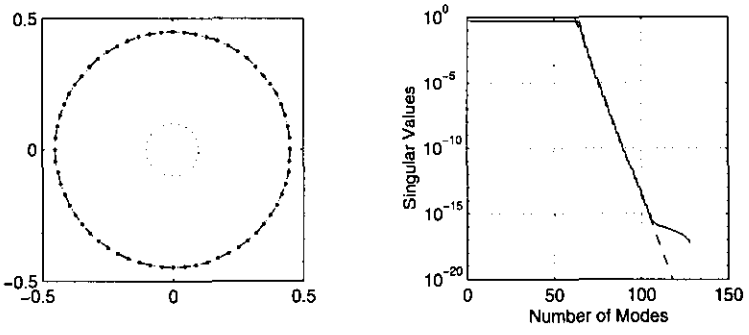

FIGURE 3. $\Omega = B_{0.45} \setminus \bar{B}_{0.1}$ with Cauchy data on $\partial B_{0.45}$ and its corresponding singular values in Example 4.4.

EXAMPLE 4.4. For numerical justifications, we first choose $R = 0.45$ and $r = 0.20$. Figure 2 presents the exponentially decaying singular values, whose decaying rate is approximately 0.6409. By the theoretical result in Theorem 4.3, the decaying rate should be $(r/R)^{1/2} = 0.6667$, since there are two modes $(\bar{\sigma}_r^m, \bar{\varphi}_r^m)$ and $(\bar{\varsigma}_r^m, \bar{\psi}_r^m)$ with same singular value $\bar{\mu}_r^m$. For the case of another ratio of R and r, we consider $R = 0.45$ and $r = 0.10$. Then we expect the decaying rate of the singular values to be 0.4714. Figure 3 presents the singular value distribution whose decaying rate is approximately 0.4394.

In section 3, we commented that the choice of the norm in the target space of $\mathcal{C}$ is not important. The following remark shows the asymptotic

behavior of the singular values of $\mathcal{C} : L^2(\partial\Omega) \to H^1(\partial B_R) \times L^2(\partial B_R)$ is essentially same as that of $\mathcal{C} : L^2(\partial\Omega) \to L^2(\partial B_R) \times L^2(\partial B_R)$.

REMARK 4.5. Under the same assumption in Lemma 4.1 with $R < 1/\sqrt{2}$, the singular values of

$$\mathcal{C} : L^2(\partial\Omega) \to H^1(\partial B_R) \times L^2(\partial B_R)$$

decay exponentially. That is, the singular values $\{\tilde{\mu}_R^m, \tilde{\mu}_r^m\}_{m\geq 0}$ have the following asymptotic behavior,

$$\tilde{\mu}_R^m = O(1) \quad \text{and} \quad \tilde{\mu}_r^m = O\left(\left(\frac{r}{R}\right)^m\right). \tag{4.8}$$

PROOF. By the analogous argument in Theorem A.1, we can obtain

$$\tilde{\mu}_R^0 = \bar{\mu}_R^0, \quad \tilde{\mu}_r^0 = \bar{\mu}_r^0,$$

$$\tilde{\mu}_R^m = \frac{\tilde{\tau}_m}{\sqrt{1+\tilde{c}_m^2}}\sqrt{1+\tilde{c}_m^2\left(\frac{r}{R}\right)^{2m+1} - 2\tilde{c}_m\left(\frac{r}{R}\right)^{m+\frac{1}{2}}\frac{(1-R^2)m^2-R^2}{(1+R^2)m^2+R^2}},$$

$$\tilde{\mu}_r^m = \frac{\tilde{\tau}_m}{\sqrt{1+\tilde{c}_m^2}}\sqrt{\tilde{c}_m^2+\left(\frac{r}{R}\right)^{2m+1} + 2\tilde{c}_m\left(\frac{r}{R}\right)^{m+\frac{1}{2}}\frac{(1-R^2)m^2-R^2}{(1+R^2)m^2+R^2}},$$

where $\tilde{\tau}_m = \frac{1}{2}\sqrt{(1+R^2)+(R/m)^2}$ and $\tilde{c}_m$ is a solution of

$$x^2 - \left((R/r)^{m+1/2} - (r/R)^{m+1/2}\right)\left(\frac{(1+R^2)m^2+R^2}{(1-R^2)m^2-R^2}\right)x - 1 = 0. \tag{4.9}$$

Solving (4.9) and choosing the negative solution, we get

$$\tilde{c}_m = -\frac{(1+R^2)m^2+R^2}{(1-R^2)m^2-R^2}\left(\frac{r}{R}\right)^{m+1/2} + \frac{\frac{8(m^2R^2+R^2)}{m^2-R^4(m+1/m)^2}\left(\frac{r}{R}\right)^{m+1/2}\left(1+\left(\frac{r}{R}\right)^{2m+1}\right)^{-1}}{1+\sqrt{1-\frac{16m^2R^2(1+m^2)}{((1+R^2)m^2+R^2)^2\left(\left(\frac{r}{R}\right)^{m+1/2}+\left(\frac{R}{r}\right)^{m+1/2}\right)^2}}},$$

which implies $\tilde{c}_m = O((r/R)^m)$. Thus we have

$$\tilde{\mu}_R^m = \frac{1}{2}\sqrt{\frac{(1+R^2)+(R/m)^2}{1+O\left((r/R)^{2m}\right)}}\sqrt{1+O\left(\left(\frac{r}{R}\right)^{2m}\right)},$$

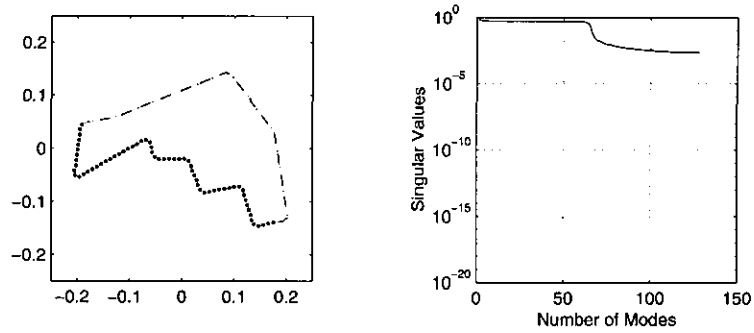

FIGURE 4. Singular values of the mixed boundary value problem with Dirichlet data on dark dotted and Neumann data on dash-dotted boundary in Example 5.1.

which proves the first part of (4.8). On the other hand, $\tilde{\mu}_r^m$ has the following asymptotic behavior

$$\tilde{\mu}_r^m = \frac{1}{2}\sqrt{\frac{(1+R^2)+(R/m)^2}{1+O\left((r/R)^{2m}\right)}}\, O\left(\left(\frac{r}{R}\right)^m\right),$$

which proves the second part of (4.8). □

5. Numerical computations and conclusion

In the previous section, we found that the singular values of the Cauchy operator are of order $O\left((r/R)^m\right)$ in an annular domain $\Omega = B_R \setminus \bar{B}_r$. Thus the operator becomes exponentially singular as the mode number m grows. We now compare numerically computed singular values of well-conditioned and those of ill-conditioned problems.

A special case of Cauchy problem is a mixed boundary value problem where the boundary is composed of a disjoint union of non-empty Dirichlet boundary and Neumann boundary, $\partial\Omega = \Gamma_D \cup \Gamma_N$. It is well-known that the mixed boundary value problem is well-conditioned and there is no loss of significance of data in obtaining the charge density by solving (2.2). The following example shows the singular values of the mixed boundary value problem and the Cauchy problem.

EXAMPLE 5.1. There exist 128 equally spaced points along the boundary of the ameba-shaped domain. In Figure 4, 64 Dirichlet data have

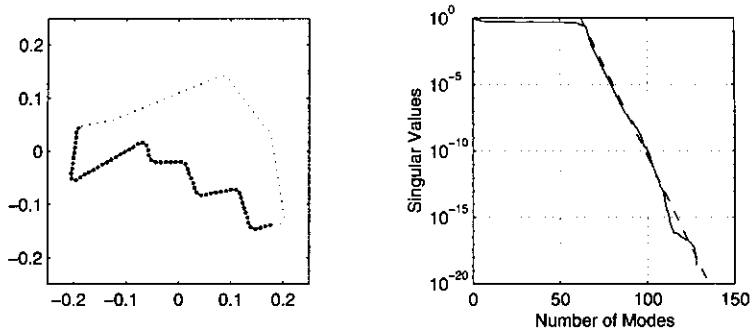

FIGURE 5. Singular values of Cauchy operator with Cauchy data on the dark dotted boundary in Example 5.1.

been specified on the lower part and 64 Neumann data on the upper part. In Figure 5, 64 pairs of Dirichlet and Neumann data have been given on the lower part of the the boundary. The singular values of the well-conditioned problem are bounded above and below as shown in Figure 4, meanwhile, Figure 5 shows the ill-conditioned Cauchy problem has exponentially small singular values.

The singular values of the Cauchy problem in Example 5.1 decay exponentially. We has already found a similar pattern of the singular values for the case of annulus in Example 4.4, which can be easily understood if one knows that oscillatory boundary data $\sin(m\theta)$ decays like $(r/R)^m$ in an annulus. Also a harmonic function which is oscillatory as $\sin(mx)$ in x-direction decays like e^{-my} in y-direction from the boundary, which makes exponential decay of singular values in planar domain. Although the singular vectors and singular values depend on the geometry of the domain, it is easy to see that highly oscillatory boundary data vanishes exponentially faster and the corresponding singular values are exponentially smaller than slowly varying boundary data. Thus, it is not hard to guess that in general domains, the singular values corresponding to highly oscillatory modes decay exponentially as mode number grows.

With the aid of the profile of singular value distribution, we are now ready to solve the Cauchy problem (2.8)

$$C[\sigma] = h$$

where $h = (f, g)^T$ is the measured Cauchy data that contains an inevitable measurement error. In order to invert the Cauchy operator C,

the natural pseudo-inverse is considered:

$$\sigma = \sum_{j \in J} \frac{1}{\mu_j} \langle h, \varphi_j \rangle \, \sigma_j, \tag{5.1}$$

where $\{(\mu_j, \sigma_j, \varphi_j)\}_{j \in J}$ are the singular system of $\mathcal{C}$. In case of exponentially decaying singular values such as in Figure 5, the solution obtained by (5.1) contains exponentially amplified error. Thus, it is not a good idea to use all the possible modes if the system has near zero singular values. In the following examples, we apply pseudo-inverse method with spectral cutoff to solve the Cauchy problems with input data containing various size of random noise. Here, the spectral cutoff means that only singular values bigger than some cutoff value are used in (5.1).

EXAMPLE 5.2. Cauchy data have been specified along the dark dotted boundary of the ameba-shaped domain shown in the upper left part of Figure 6. The lower left figure shows the singular values of the Cauchy matrix when the number of Cauchy data pairs are (A) 16, (B) 32, and (C) 64, respectively. We can see that the rate of decay is almost identical to all of three cases, however, the smallest singular values are 10^{-10} in case (A), 10^{-15} in case (B), and less than 10^{-16} in case (C). We are trying to solve the Cauchy problem using Cauchy data of known function in order to demonstrate how the small singular vectors effect the solution of Cauchy problem. For this numerical computation, Dirichlet and Neumann values of known harmonic function $u(x, y) = x + y$ with specified random noise have been tabulated on 64 Cauchy boundary points. The rightmost figure shows the relative L^2 error of computed $\sigma(y)$ as a function of used number of modes to invert the Cauchy operator. The dotted line represents the relative error when the Cauchy data contains noise of level $10^{-5}$and the dash-dotted line and the solid line when the level is 10^{-10} and 10^{-15}, respectively.

One may misconceive that more accurate solution to the Cauchy problem can be obtained by using more eigenfunctions in the inversion process. It is possible only when the problem is well-conditioned and the singular values of the operator are bounded below, however, the Cauchy problem is not the case. The best solution was achieved when 79 eigenmodes are involved in (5.1) for the Cauchy data of noise level 10^{-5} and the minimum error was marked with triangles in Figure 6. Similarly, 100 and 112 modes are the best choices for the data of noise level 10^{-10} and 10^{-15} which are marked with squares and circles, respectively. Then, a

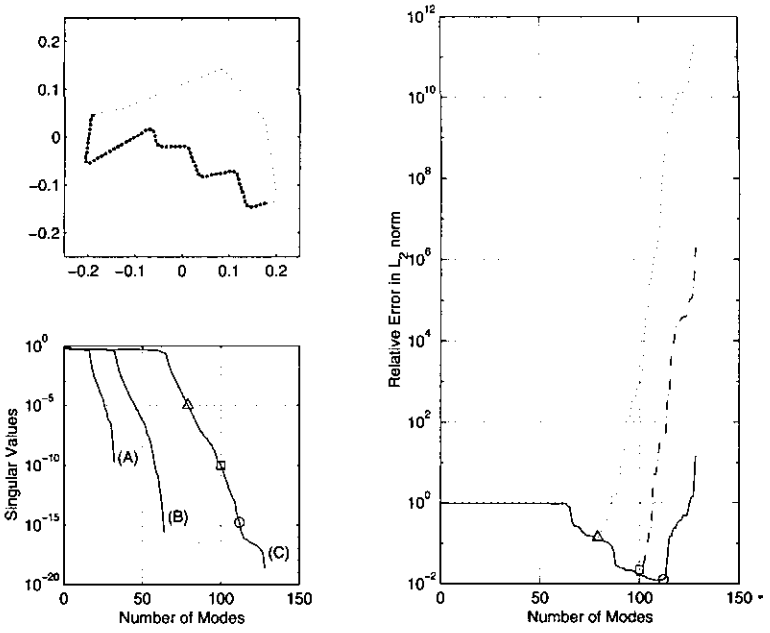

FIGURE 6. An ameba-shaped domain and the singular values are drawn when (A) 16, (B) 32, and (C) 64 Cauchy data pairs are used in Example 5.2. The rightmost plot shows relative errors computing $\sigma(y)$ with 64 Cauchy data pairs. The dotted, dash-dotted, and solid lines represent the reconstruction errors and a triangle, a square, and a circle marks the best obtainable errors for the data with $10^{-5}, 10^{-10}, 10^{-15}$ noise level.

natural question would be how many modes should be used to get the best reconstructed solution. Once the error size $\mathcal{E}$ of the input data is known, the optimal number M_{opt} of modes that will be utilized in (5.1) for the Cauchy problem is

$$[\tau(\Omega)]^{M_{opt}} \lesssim \mathcal{E} \tag{5.2}$$

where $\tau(\Omega)$ is the decaying rate of singular values.

The pseudo-inverse method with spectral cutoff gives a near optimal solution, however, obtaining complete eigensystem is computationally expensive and it is sometimes not practical. In such cases, the number of discretization points in Cauchy inversion should be restricted since condition number of the Cauchy matrix increases as the number of points on the Cauchy boundary increases as we can see in the lower left plot in

Figure 6. The maximum number of discretization M_{dis} should be

$$[\tau(\Omega)]^{M_{dis}} \lesssim \mathcal{E} \tag{5.3}$$

when a direct inversion method is applied without using pseudo-inverse.

Thus, it is crucial to investigate the decaying rate τ of the Cauchy operator $\mathcal{C}$ to design an optimal numerical solver which does not use expensive singular value decomposition. The decaying rate τ is, of course, a function of geometry and it is difficult to get an exact formula. However, it is possible to estimate the rate in general domains using simple geometrical parameters and readers interested in the geometric dependence of $\tau(\Omega)$ will find some results in our forthcoming paper.

Appendix A. Singular system of $\mathcal{C}$ into $L^2(\partial B_R) \times L^2(\partial B_R)$

THEOREM A.1. *Under the same assumption in Lemma 4.1 with $R < 1$, the singular system of $\mathcal{C} : L^2(\partial\Omega) \to L^2(\partial B_R) \times L^2(\partial B_R)$ is composed of the following six families:*

$$\left\{\left(\bar{\mu}_R^0 := \frac{\beta_0}{\alpha_0},\ \bar{\sigma}_R^0 := \frac{\sigma_R^0 + c_0\sigma_r^0}{\alpha_0},\ \bar{\varphi}_R^0 := \frac{(R\log R)\varphi_R^0 + c_0 d_0 \varphi_r^0}{\beta_0}\right)\right\},$$

$$\left\{\left(\bar{\mu}_R^m := \frac{\tau_m\beta_m}{\alpha_m},\ \bar{\sigma}_R^m := \frac{\sigma_R^m + c_m\sigma_r^m}{\alpha_m},\ \bar{\varphi}_R^m := \frac{\varphi_R^m + c_m(r/R)^{m+\frac{1}{2}}\varphi_r^m}{\beta_m}\right)\right\},$$

$$\left\{\left(\bar{\mu}_R^m := \frac{\tau_m\beta_m}{\alpha_m},\ \bar{\varsigma}_R^m := \frac{\varsigma_R^m + c_m\varsigma_r^m}{\alpha_m},\ \bar{\psi}_R^m := \frac{\psi_R^m + c_m(r/R)^{m+\frac{1}{2}}\psi_r^m}{\beta_m}\right)\right\},$$

$$\left\{\left(\bar{\mu}_r^0 := \frac{\gamma_0}{\alpha_0},\ \bar{\sigma}_r^0 := \frac{-c_0\sigma_R^0 + \sigma_r^0}{\alpha_0},\ \bar{\varphi}_r^0 := \frac{-c_0(R\log R)\varphi_R^0 + d_0\varphi_r^0}{\gamma_0}\right)\right\},$$

$$\left\{\left(\bar{\mu}_r^m := \frac{\tau_m\gamma_m}{\alpha_m},\ \bar{\sigma}_r^m := \frac{-c_m\sigma_R^m + \sigma_r^m}{\alpha_m},\ \bar{\varphi}_r^m := \frac{-c_m\varphi_R^m + (r/R)^{m+\frac{1}{2}}\varphi_r^m}{\gamma_m}\right)\right\},$$

$$\left\{\left(\bar{\mu}_r^m := \frac{\tau_m\gamma_m}{\alpha_m},\ \bar{\varsigma}_r^m := \frac{-c_m\varsigma_R^m + \varsigma_r^m}{\alpha_m},\ \bar{\psi}_r^m := \frac{-c_m\psi_R^m + (r/R)^{m+\frac{1}{2}}\psi_r^m}{\gamma_m}\right)\right\},$$

where $m \geq 1$ and $d_0 = \sqrt{r/R}\sqrt{1 + [R\log R]^2}$,

$$\beta_0 = \sqrt{c_0^2\,(r/R) + \left[R\log R\left(1 + c_0\sqrt{r/R}\right)\right]^2},$$

$$\gamma_0 = \sqrt{(r/R) + \left[R\log R\left(c_0 - \sqrt{r/R}\right)\right]^2}.$$

Here c_0 is a solution of

$$x^2 - \sqrt{r/R}\left(1 + [R\log R]^{-2} - (R/r)\right)x - 1 = 0, \tag{A.1}$$

c_m is a solution of

$$x^2 - \left((R/r)^{m+\frac{1}{2}} - (r/R)^{m+\frac{1}{2}}\right)\left(\frac{m^2+R^2}{m^2-R^2}\right)x - 1 = 0, \tag{A.2}$$

and α_m, β_m, γ_m and τ_m are given by

$$\alpha_m = \sqrt{1+c_m^2}, \qquad \tau_m = \frac{1}{2}\sqrt{1+\left(\frac{R}{m}\right)^2},$$

$$\beta_m = \sqrt{1 + c_m^2\left(\frac{r}{R}\right)^{2m+1} - 2c_m\left(\frac{r}{R}\right)^{m+\frac{1}{2}}\frac{m^2-R^2}{m^2+R^2}},$$

$$\gamma_m = \sqrt{c_m^2 + \left(\frac{r}{R}\right)^{2m+1} + 2c_m\left(\frac{r}{R}\right)^{m+\frac{1}{2}}\frac{m^2-R^2}{m^2+R^2}}.$$

PROOF. From (4.2), it is easy to show that

$$\mathcal{C}[\bar\sigma_R^0] = \bar\mu_R^0\bar\varphi_R^0, \qquad \mathcal{C}[\bar\sigma_R^m] = \bar\mu_R^m\bar\varphi_R^m, \qquad \mathcal{C}[\bar\varsigma_R^m] = \bar\mu_R^m\bar\psi_R^m,$$
$$\mathcal{C}[\bar\sigma_r^0] = \bar\mu_r^0\bar\varphi_r^0, \qquad \mathcal{C}[\bar\sigma_r^m] = \bar\mu_r^m\bar\varphi_r^m, \qquad \mathcal{C}[\bar\varsigma_r^m] = \bar\mu_r^m\bar\psi_r^m.$$

Since $\Sigma = \{\sigma_R^0, \sigma_R^m, \varsigma_R^m, \sigma_r^0, \sigma_r^m, \varsigma_r^m\}_{m\geq 1}$ in (4.3) is an orthonormal system in $L^2(\partial\Omega)$,

$$\bar\Sigma := \{\bar\sigma_R^0, \bar\sigma_R^m, \bar\varsigma_R^m, \bar\sigma_r^0, \bar\sigma_r^m, \bar\varsigma_r^m\}_{m\geq 1}$$

can be also shown to be an orthonormal system in $L^2(\partial\Omega)$ due to its own construction.

To complete the proof, we only need show that

$$\bar\Psi := \{\bar\varphi_R^0, \bar\varphi_R^m, \bar\psi_R^m, \bar\varphi_r^0, \bar\varphi_r^m, \bar\psi_r^m\}_{m\geq 1}$$

is an orthonormal system in $Y := L^2(\partial B_R) \times L^2(\partial B_R)$.

With the aid of (4.5) and the definitions of β_0 and γ_0, we have

$$\|\bar\varphi_R^0\|_Y^2 = \frac{1}{\beta_0^2}\left(c_0^2\left(\frac{r}{R}\right) + (R\log R)^2\left(1 + c_0\sqrt{\frac{r}{R}}\right)^2\right) = 1,$$

$$\|\bar\varphi_r^0\|_Y^2 = \frac{1}{\gamma_0^2}\left(\left(\frac{r}{R}\right) + (R\log R)^2\left(c_0 - \sqrt{\frac{r}{R}}\right)^2\right) = 1.$$

Similarly, by (4.6) and definitions of β_m and γ_m, we easily see that

$$\|\bar\varphi_R^m\|_Y^2 = \|\bar\psi_R^m\|_Y^2 = \|\bar\varphi_r^m\|_Y^2 = \|\bar\psi_r^m\|_Y^2 = 1.$$

For the orthogonality of $\bar{\Psi}$, from the fact that

$$\Psi = \{\varphi_R^0, \varphi_R^m, \psi_R^m, \varphi_r^0, \varphi_r^m, \psi_r^m\}_{m\geq 1}$$

in (4.4) is an almost orthogonal family except (4.5) and (4.6), we only need to check

$$\langle \bar{\varphi}_R^0, \bar{\varphi}_r^0 \rangle_Y = \langle \bar{\varphi}_R^m, \bar{\varphi}_r^m \rangle_Y = \langle \bar{\psi}_R^m, \bar{\psi}_r^m \rangle_Y = 0. \tag{A.3}$$

By tedious calculations using (4.5) and (4.6), we obtain

$$\langle \bar{\varphi}_R^0, \bar{\varphi}_r^0 \rangle_Y = -\frac{(R\log R)^2}{\beta_0\gamma_0}\sqrt{\frac{r}{R}}\left(c_0^2 - \sqrt{\frac{r}{R}}\left(1 + (R\log R)^{-2} - \frac{R}{r}\right)c_0 - 1\right),$$

$$\begin{aligned}\langle \bar{\varphi}_R^m, \bar{\varphi}_r^m \rangle_Y &= \langle \bar{\psi}_R^m, \bar{\psi}_r^m \rangle_Y \\ &= \frac{(\frac{r}{R})^{m+\frac{1}{2}}}{\beta_m\gamma_m}\frac{m^2 - R^2}{m^2 + R^2} \\ &\quad \times \left(c_m^2 - \left(\left(\frac{R}{r}\right)^{m+\frac{1}{2}} - \left(\frac{r}{R}\right)^{m+\frac{1}{2}}\right)\left(\frac{m^2+R^2}{m^2-R^2}\right)c_m - 1\right).\end{aligned}$$

Since we have chosen c_0 and c_m as the solution of (A.1) and (A.2), respectively, (A.3) is proved. This completes the proof. □

References

[1] J. Cheng, Y. Hon, and M. Yamamoto, *Stability in line unique continuation of harmonic functions: general dimensions*, Inverse and Ill-posed Problems **6** (1998), no. 4, 319–326.

[2] A. Greenbaum, L. Greengard, and G. McFadden, *Laplace's equation and the Dirichlet-Neumann map in multiply connected domains*, J. Comput. Phys. **105** (1993), no. 2, 267–278.

[3] C. Groetsch, *The Theory of Tikhonov Regularization for Fredholm Equations of the First Kind*, Pitman, Boston, 1984.

[4] Y. Hon and T. Wei, *Backus-Gilbert algorithm for a Cauchy problem of Laplace equation*, Inverse Problems **17** (2001), 261–271.

[5] L. Landweber, *An iteration formula for Fredholm integral equations of the first kind*, Am. J. Math. **73** (1951), 615–624.

[6] V. Morozov, *Choice of parameter for the solution of functional equations by the regularization method*, Sov. Math. Doklady **8** (1967), 1000–1003.

[7] K. Onishi and Q. Wang, *Numerical solutions of the Cauchy problem in potential and elastostatics*, Inverse problems and related topics (Kobe, 1998), Chapman & Hall/CRC (2000), pp. 115–132, Boca Raton, FL.

[8] M. Shelley, *A case of singularity formation in vortex sheet motion studied by a spectrally accurate method*, J. Fluid Mech. **224** (1992), 493–526.

[9] A. Sidi and M. Israeli, *Quadrature methods for periodic singular and weakly singular Fredholm integral equations*, J. Sci. Comput. **3** (1988), 201–231.

[10] A. Tikhonov, *Regularization of incorrectly posed problems*, Sov. Doklady **4** (1963), 1624–1627.

June-Yub Lee
Department of Mathematics
Ewha Womans University
Seoul 120-750, Korea
E-mail: jylee@math.ewha.ac.kr

Jeong-Rock Yoon
School of Mathematics
Korea Institute for Advanced Study
Seoul 130-012, Korea
E-mail: jryoon@numer.kaist.ac.kr